PII: S0043-1354(01)00159-2

Wat. Res. Vol. 35, No. 18, pp. 4331–4338, 2001

Printed in Great Britain
0043-1354/01/$ - see front matter

PERGAMON
www.elsevier.com/locate/watres

RESIDUE CHARACTERISTICS AND PORE DEVELOPMENT OF PETROCHEMICAL INDUSTRY SLUDGE PYROLYSIS

HUNG-LUNG CHIANG[1]*, CHING-GUAN CHAO[1], C. Y. CHANG[2], C. F. WANG[2] and P. C. CHIANG[3]

[1] Department of Environmental Engineering, Fooyin Institute of Technology, Kaoshsiung Hsien, Taiwan, ROC; [2] Department of Nuclear Science, National Tsing Hua University, Hsinchu, Taiwan and [3] Graduate Institute of Environmental Engineering, National Taiwan University, Taipei, Taiwan, ROC

(First received 13 October 2000; accepted in revised form 12 March 2001)

Abstract—Petrochemical industry bio-sludge was pyrolyzed to investigate the composition and pore size distribution of pyrolytic residue. Results indicated that the carbon, nitrogen, and hydrogen concentrations could be reduced after an increase in pyrolytic temperature. The trace element analysis indicated that Al, Ca, Fe, Mg, K, Cu, Sr, and Sb concentrated during the pyrolytic process. When forty grams of pre-dried sludge were pyrolyzed at various pyrolytic temperatures, the transfers from the gas phase to liquid phase to residue were from 21.2 to 36.0%, from 49.0 to 70.0%, and from 8.3 to 16.5%. Results of the pore size distribution examination indicated that the mesopore had the greatest effect on the bio-sludge pyrolysis. The optimal pyrolytic temperatures and times were approximately 800°C for 30 min and 900°C for 10 min. The conceptual model can reasonably explain the pore structure development during the pyrolysis process.

Key words—biosludge, pyrolysis, pore size distribution, element composition, petrochemical industry

INTRODUCTION

In Taiwan, 74,150 ton of sludge were produced from industrial parks in 1998 (Taiwan EPA, 1999). Sludge was treated by landfill (33.9%), compost (1.2%), incineration (27.9%), recycled for brick (37.0%), and solidified (0.04%) (Taiwan EPA, 1999). A great deal of money was required for disposal. Over one-third of the sewage sludge was recycled. According to baseline information, sludge can be recycled from the incineration treatment process in Taiwan.

The reuse of digested sludge on farmland is limited by the uptake capacity of the soil and the high concentration of toxic organic constituents and heavy metals (Dumpelmann *et al.*, 1991). Additionally, in many countries like Taiwan, landfill treatment is limited by land cost and insufficient land. Incineration provides a large volume reduction and results in improved energy efficiency, although the scrubbing cost of the exhaust gas is high. The pyrolysis of sewage sludge in an oxygen-free atmosphere in fluidized beds has been proposed by Kaminsky (1989). Work that has been carried out by Piskorz *et al.* (1986) achieved high liquid yields. These were obtained by a short residence time (0.55 s) and medium temperature (450°C). Bayer and Kutubuddin (1987) and Briddle (1982) used rotary kilns at low temperatures (250–450°C) to generate maximum liquid products. Pyrolytic residues, i.e. the char, can be used as an adsorbent if pyrolyzed under controlled conditions or with some chemical treatment (Chiang and You, 1987).

Kim *et al.* (1996) investigated the technical feasibility of converting paint sludge to activated char and reusing the char in paint solvent adsorption. Lu *et al.* (1995) investigated the surface area development of sewage sludge during the pyrolytic process.

In this work, we focused on the elemental composition and pore size distribution of the pyrolytic residue of sludge, which was taken from a petrochemical wastewater treatment plant and pyrolyzed in a nitrogen atmosphere. Various temperatures and times were used. The chemical composition, BET (Brubauer, Emmett, and Teller) surface area, and residue pore size distribution were measured.

EXPERIMENTAL

Raw material

The sludge sample was obtained from a petrochemical wastewater treatment plant in Kaohsiung, Taiwan. The

*Author to whom all correspondence should be addressed. Fax: +886-7-7829117; e-mail: hlchiang@mail.fy.edu.tw

sludge cake of about 300 kg was sampled at one time to avoid varying sludge characteristics. Sludge was stored at 4°C until pyrolyzed. Two kilograms of the sludge sample were dried in an oven at 105°C for 24 h in each run. Raw activated sludge cakes had a total solids (TS) content of 12.7 ± 1.2 wt% and a volatile solids (VS) concentration of 73.5 ± 4.3 wt%. The sludge cake was conditioned and dried at 378 K. Carbon, oxygen, hydrogen, nitrogen and sulfur concentrations were 39.0, 24.4, 5.70, 4.75, and 1.18%.

Pyrolysis process

Pyrolysis was carried out in an isothermal reactor heated by a horizontal electric furnace. At the beginning of each run, 40 g of pretreated sewage sludge (irregularly spherical shape, diameter: 1.0–1.5 cm) was placed in the middle of a quartz tube internal diameter (I.D.) 30 mm and length 70 cm). High purity (99.995%) nitrogen was used as the purging gas, which flowed through the sample bed at 2 L/min. The reactor was heated to the designated temperature at 15 K/min. The pyrolysis temperatures and the sample residence times varied from 400 to 900°C (400, 500, 600, 700, 800, and 900°C) and from 3 to 90 min (3, 5, 10, 15, 20, 25, 30, 60, and 90 min). Each experiment was run with one pyrolytic temperature at four to five different pyrolytic times. After pyrolysis, the reactor was cooled down to room temperature before the pyrolysis residue was removed for quantification and characterization. The amount of sludge pyrolysis residue was weighed on an analytical balance (Mettler–Toledo, model AB204-S, Switzerland, weighing limit is less than 0.1 mg).

Chemical compositions of residue

To obtain a stabilized pyrolysis residue weight, 30 min was chosen as the optimal pyrolysis time in these experiments. The nitrogen, carbon, hydrogen, and oxygen constituents were analyzed with an element analyzer (Heraeus CHN–O Rapid Element analyzer, USA). Sulfur and chloride concentrations were measured with the Tacussel Coloumax 78 (USA) element analyzer. Sulfanilic acid and 1-chloro-2, 4-dinitrobenzene were used as standards.

The pyrolysis residue was digested with a mixture of $HNO_3 : HClO_4 : HF$ in a 3 : 5 : 2 proportion. ICP-AES and ICP-MS analyzed the sludge pyrolysis residue for Sr, As, Cr, Ba, Mn, Ni, V, Se, Cd, Sb, Al, Ca, Fe, Na, Mg, K, S, Zn, Pb, and Cu. Analysis was performed on five samples in duplicate for quality assurance and quality control.

Pore size distribution of pyrolytic residue

The pyrolytic residue samples were placed in a vacuum oven (10^{-2}–10^{-3} mmHg, 105°C) and dried for 24 h. The physical characteristics of the pyrolytic residues, including specific surface area, micropore area, total pore volume, micropore volume, pore size distribution and pore diameter were measured with N_2 (g) adsorption (ASAP 2010 Pore Structure Analyzer, Micromeritrics Inc., USA) at 77 K with liquid N_2. The BET surface area, micropore surface area, total pore volume, and micropore volume were calculated by the BET method (Brubauer *et al.*, 1938), the BET surface area minus external surface area BJH method (Barrett *et al.*, 1951), the *t*-plot method (Lippens and de Boer, 1965) and the Harkins–Jura method (Harkins and Jura, 1944).

RESULTS AND DISCUSSION

Element compositions of sludge and residue

Major element composition of sludge and residue. The oven dried sludge and the pyrolytic residues were analyzed for carbon, hydrogen, nitrogen, oxygen, sulfur, and chlorine. Constituents are listed in Fig. 1. Chlorine was not detected in any residue or sludge. The percentage of each element in the pyrolysis residue was less than that of the oven-dried sludge. When pyrolytic temperatures increased, the total elemental content decreased. The rate of transformation decreased at temperatures greater than 500°C. The results also revealed that the amount of

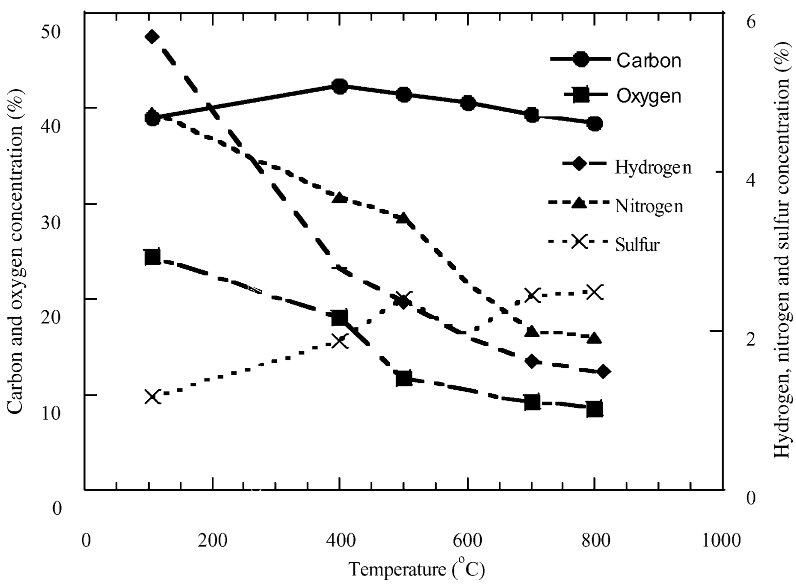

Fig. 1. Major element compositions of sludge residue at different pyrolysis temperatures.

carbon, nitrogen, hydrogen, and oxygen from the residues decreased when the pyrolysis temperature was raised from 400 to 800°C, suggesting that the carbon, nitrogen, hydrogen, and oxygen were desorbed but sulfur was not.

Trace element compositions of sludge pyrolysis residue. Results of the element composition in the sludge pyrolysis residue are summarized in Table 1. When the pyrolysis temperatures ranged from 400 to 800°C, the Al, Ca, Fe, Mg, K, Zn, Cu, Sr, Sb and Cd concentrations ranged from 20 to 33 mg/g, 23 to 40 mg/g, 8.6. to 16 mg/g, 4.2 to 7.2 mg/g, 11 to 18 mg/g, 3.6 to 5.1 mg/g, 0.05 to 0.09 mg/g, 207 to 315 μg/g, from 2.4 to 9.59 μg/g, and from 0.17 to 0.52 μg/g, respectively. Pyrolysis increased the Al, Ca, Fe, Mg, K, Cu, Sr and Sb concentrations. The Cd concentration decreased because it was volatile at temperatures higher than 600°C. The elemental compositions decreased correspondingly to the pyrolytic temperature increases. The concentrations varied in the residue because different elemental complexes (i.e. OH^-, S^{2-}, Cl^-, CO_3^{2-}, NO_3^- and SO_4^{2-}) could not be completely digested in the $HNO_3:HClO_4:HF$ solution or analyzed by ICP-AES and ICP-MS.

Mass balance of sludge pyrolysis

Water vapor and some volatile compounds (1365 g) were volatilized from the original 2000 g by a dewatering process. Resultant dry sludge was 635±61 g. Forty grams of the dry sludge produced 19.6 to 28.0 g liquid product (water and crude oil) and a pyrolyzed sludge residue of 6.0 to 3.3 g. The dry sludge was transformed into a liquid phase (water and crude oil), solid phase (sludge residue), and gas phase (water vapor, CO, CO_2, H_2, methanol, and other volatile compounds) by the pyrolysis process. The dry sludge that was pyrolyzed and transferred into the gas phase yielded 14.4, 9.8, 9.2, 8.5 and 9.1 g when pyrolyzed at 400, 500, 600, 700 and 800°C, respectively. Elements of the pyrolysis sludge residue (C, H, N, O, S, Cl, Sr, As, Cr, Ba, Mn, Ni, V, Se, Cd, Sb, Al, Ca, Fe, Na, Mg, K, Zn, Pb, and Cu) decreased from 75.1 to 54.7% (Fig. 2).

Surface development of pyrolytic residue

Physical characteristics. Table 2 details the surface characteristics of the pyrolytic residue. Increasing pyrolytic temperatures heightened the BET surface area. Data indicate that the highest BET pyrolytic residue surface area was obtained when the temperature and time were in the vicinity of 800°C and 30 min.

Figure 3 shows that the nitrogen adsorption isotherm (77 K) of the sludge pyrolyzed at various temperatures are typically type II, indicating a

Table 1. ICP-AES and ICP-MS analyze element compositions of sludge pyrolysis residue[a]

Temperature (°C)	Al	Ca	Fe	Na	Mg	K	S	Zn	Pb	Cu
400	20±12[b]	23±12	8.6±5.8	13±7.1	4.2±2.6	11±8.9	18±5.3	3.7±2.0	0.03±0.03	0.05±0.03
500	21±8.7	21±13	8.9±5.1	16±9.1	4.2±2.1	14±10	24±9.5	3.6±1.2	0.05±0.05	0.05±0.02
600	24±7.5	29±9.1	10±4.9	18±10	4.8±2.2	14±8.3	24±9	4.5±1.5	0.03±0.03	0.07±0.02
700	25±7.1	32±9.2	11±5.0	17±9.3	5.4±2.0	14±10	21±4.7	4.9±1.7	0.02±0.01	0.07±0.04
800	33±6.5	40±7.8	16±4.7	17±9.7	7.2±2.0	18±11	20±2.1	5.1±1.2	0.03±0.04	0.09±0.03
	Sr	As	Cr	Ba	Mn	Ni	V	Se	Cd	Sb
400	207±101	124±142	119±83.1	153±137	167±85.5	87.7±73.4	192±214	547±657	0.52±0.24	2.4±2.8
500	217±70.5	148±100	162±157	140±116	184±54	194±238	236±150	658±458	0.45±0.17	3.84±5.01
600	274±82.3	49.1±34.2	92.9±49.1	136±47.8	252±82.8	82.3±45.3	82.9±60.8	194±155	0.53±0.14	3.81±6.19
700	272±86.4	111±120	124±63.5	149±77.7	210±69.4	83.3±37.7	174±193	490±560	0.38±0.16	6.61±8.25
800	315±61.1	82.8±58.5	155±82.7	151±19.9	279±62.2	124±40.4	131±101	323±280	0.17±0.20	9.59±11.5

[a] Analysis sample number is 7. The unit of Al, Ca, Fe, Na, Mg, K, S, Zn, Pb and Cu is mg/g; that of Sr, As, Cr, Ba, Mn, Ni, V, Se, Cd and Sb is μg/g.
[b] Standard deviation.

Table 2. Pore size distribution of sludge pyrolytic residue

Temperature (°C)	Time (min)	BET surface area (m^2/g)	Average pore diameter (Å)	Pore size distribution (cm^3/g)				Percentage of pore size (%)			Micropore area (m^2/g)
				Macropore	Mesopore	Micropore	Total pore volume	Macropore	Mesopore	Micropore	
400	15	2.77	92.58	0.0034	0.0061	0.0002	0.0098	35.1	62.7	2.2	ND
	25	5.12	71.47	0.0030	0.0092	0.0002	0.0124	24.4	74.2	1.4	ND
	60	7.23	55.00	0.0022	0.0091	0.0003	0.0116	19.0	78.5	2.5	ND
	90	10.69	61.08	0.0171	0.0145	0.0012	0.0328	51.9	44.3	3.8	ND
500	3	5.19	36.91	0.0007	0.0047	0.0004	0.0058	12.3	81.1	6.6	ND
	10	6.69	57.09	0.0019	0.0092	0.0005	0.0117	16.0	79.3	4.6	ND
	20	10.51	60.56	0.0029	0.0151	0.0010	0.0190	15.1	79.5	5.5	ND
	30	13.26	54.10	0.0030	0.0181	0.0005	0.0216	13.8	83.8	2.4	ND
	60	9.32	58.32	0.0021	0.0149	0.0009	0.0179	11.9	83.1	5.0	ND
600	3	1.42	54.90	0.0004	0.0018	0.0001	0.0023	16.1	79.8	4.2	ND
	10	7.26	84.11	0.0057	0.0148	0.0005	0.0210	27.3	70.3	2.4	ND
	15	10.41	59.13	0.0028	0.0146	0.0011	0.0185	15.2	79.0	5.8	ND
	25	10.14	60.35	0.0031	0.0146	0.0010	0.0187	16.5	78.1	5.4	ND
	30	5.18	92.34	0.0063	0.0117	0.0002	0.0181	34.6	64.4	1.1	ND
	60	5.97	83.9	0.0066	0.0115	0.0002	0.0184	36.1	62.8	1.2	ND
700	3	4.31	85.3	0.0045	0.0125	0.0004	0.0174	25.9	71.8	2.3	ND
	10	6.94	70.31	0.0086	0.0134	0.0006	0.0226	38.1	59.3	2.7	ND
	15	7.47	78.1	0.0084	0.0138	0.006	0.0228	36.7	60.5	2.8	ND
	20	13.3	57.4	0.0205	0.0193	0	0.0398	51.6	48.4	0	ND
	30	8.86	80.0	0.0095	0.0171	0.0005	0.0272	35.0	63.0	2.0	ND
	60	7.86	72.31	0.0028	0.0133	0.0010	0.0171	16.3	77.8	5.9	ND
800	3	9.01	83.87	0.0090	0.0183	0.0005	0.0279	32.4	65.8	2.5	ND
	10	18.63	62.41	0.0056	0.0292	0.0012	0.0359	15.5	81.1	3.4	ND
	25	43.02	38.47	0.0075	0.0320	0.0009	0.0405	18.7	79.1	2.3	13.04
	30	37.92	55.88	0.0154	0.0460	0.0007	0.0621	24.8	74.1	1.1	11.20
	60	28.62	50.32	0.0322	0.0256	0.0010	0.0588	54.7	43.6	1.8	5.63
900	3	11.64	66.36	0.0292	0.0176	0.0011	0.0479	61.0	36.7	2.3	ND
	5	15.51	71.47	0.0104	0.0264	0.0005	0.0373	27.8	70.9	1.3	0.27
	10	40.32	32.26	0.0066	0.0248	0.0011	0.0326	20.3	76.2	3.5	13.98
	30	34.87	71.96	0.0083	0.0645	0	0.0727	11.4	88.6	0.0	ND
	60	29.80	85.34	0.0062	0.0324	0.0005	0.0391	15.9	82.9	1.3	ND

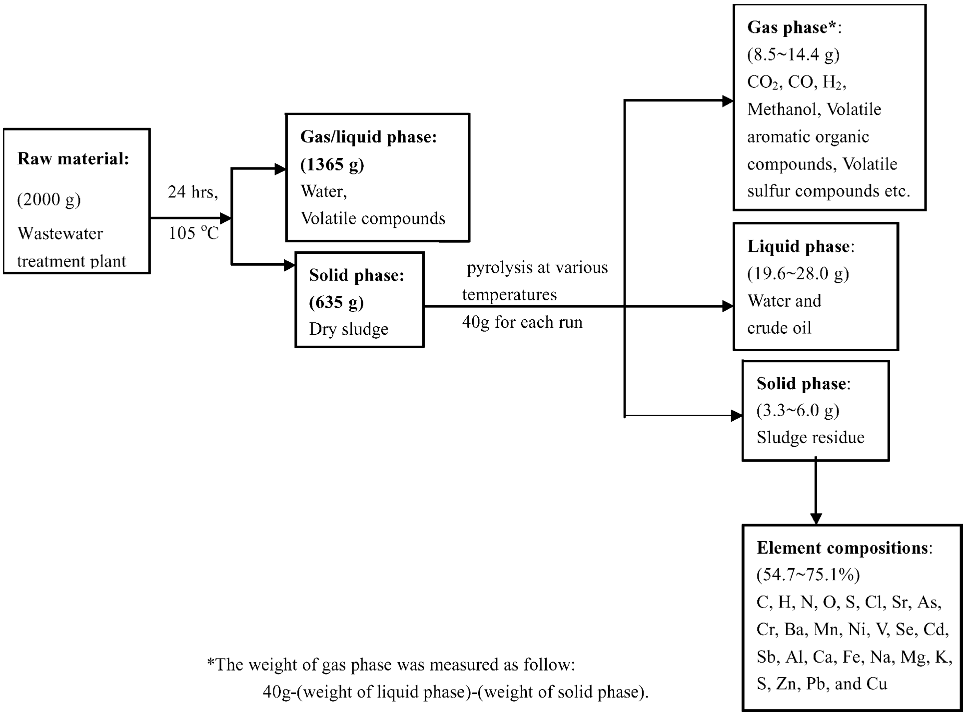

Fig. 2. Mass balance of sludge in drying and pyrolysis process.

smaller micropore structure. The amount of adsorbed nitrogen indicates the adsorption capacity of the pyrolytic residue; pyrolytic temperatures greater than 800°C correspond to a higher adsorption capacity. More mesopores and micropores are developed (Table 2).

According to the IUPAC classification, the pore can be divided into three clusters: such as a macropore (pore diameter is larger than 500 Å), mesopore (pore diameter is between 20 to 500 Å), and micropore (pore diameter is smaller than 20 Å). The results indicated that the mesopore contributed more than the macropore and micropore to the sludge pyrolytic residue. This sludge contains microorganisms, and therefore, the aggregated structure is not rigid like that of a lignin coconut shell or coal activated carbon structure. The polysaccharides are the major components of the microorganism secrete slime layer (Talaro *et al*., 1999) and produce a micropore size. In general, the cell wall of the microorganism is composed of peptidoglycans (*N*-acetyl muramic acid, *N*-acetyl glucosamine, and amino acid, etc.) (Talaro *et al*., 1999). The polysaccharide bond energy is lower than that of peptidoglycan. The polysaccharides are volatilized at the lower pyrolytic temperatures and form macropores and mesopores. When the pyrolytic temperature was higher than 700-800°C, the peptidoglycan cracked and formed the mesopore and micropore.

The results indicated that the shorter the pyrolytic time, the larger is the macropore contribution to the pore structure. The water and easier volatile molecules in the mucous membrane and cell were vaporized to generate the macropore during the initial stage of the pyrolytic process. As the pyrolytic time and temperature increased, the cell wall cracked to generate both mesopore and micropore. Figure 4 shows the pore size distribution of the pyrolytic residue. Table 2 indicates that the micropore was developed at 800 and 900°C. The process times were from 25 to 60 min, and from 5 to 10 min, respectively. When the pyrolytic time was too short, the micropore could not develop, but when the time was too long, the micropore could be destroyed. Therefore, the optimal pyrolytic times for micropore formation at 800 and 900°C were in the vicinity of 25 and 10 min.

Conceptual model of pore development. In spite of pyrolysis conditions, the pyrolysis residues inherited some physical structure from the raw materials tissue. The fact that active sludge from biological wastewater treatment is a cluster of bacteria makes it reasonable to deduce the pore characters of pyrolysis residue from bacteria cell structure. The typical aerobic heterotrophic bacteria in activated sludge are *Psudomonas* (Gram(−)), *Flavobacterium* (Gram(−)), *Bacillus* (Gram(+)), *Arthrobacter* (Gram(+)), etc (Bitton, 1999). Bacteria are small

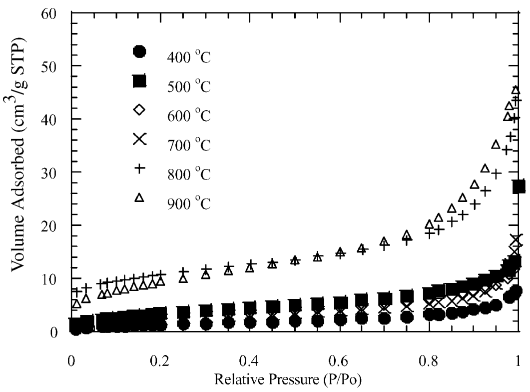

Fig. 3. Nitrogen adsorption isotherm for various pyrolytic temperatures.

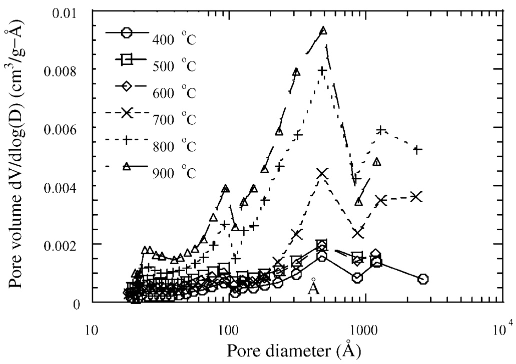

Fig. 4. Pore size distribution of sludge pyrolytic residue.

rods, cocci or filament, having a general diameter in micrometers. All bacteria, except *Mycoplasma*, have a porous, rigid and high tensile strength cell wall that consists of murein, a unique type of peptidoglycan. The bulk of the Gram (+) bacteria cell wall is a thick, homogeneous sheath of peptidoglycan ranging from 20 to 80 nm in thickness. Gram (−) bacteria have a thinner peptidoglycan ranging from 8 to 11 nm in thickness under lipid outer membrane (Talaro *et al.*, 1999).

Peptidoglycan is a polymer of disaccharides (a glycan) cross-linked by short chains of amino acids (peptides). The glycan backbone is made up of alternating molecules of *N*-acetylglucosamine (NAG) and N-acetylmuramic acid (NAM) connected by a β 1,4-glycoside bond. The 3-carbon of NAM is substituted with a lactyl ether group connected to a peptide side chain that contains amino acids differing for different species (Todar, 1999). Molecular simulation used a molecular mechanical Molecular mechanics-2 (MM2) mechanis method to calculate the size of the peptidoglycan mesh (Burkert and Allinger, 1982). The results revealed that the distance between two tetrapeptides was about 10–11 Å for both species. The distance between two glycan backbones was about 10–11 Å for *E. coli* and about 25 Å for *S. aureus*. Figure 5(c) is a schematic diagram of the peptidoglycan sheet of *S. aureus*. The thickness of a single sheet was about 10–11 Å for both *S. aureus* and *E. coli*.

Figure 5 indicates the conceptual model of pore development during the sludge pyrolysis process. The dry bacterium (Fig. 5(a)) is imaged as a tiny hollow sphere with a thick rigid murein shell. The vaporization of inner small molecular contents (water vapor, low molecular weight compounds, etc.) should crack the cell wall to form pores (Fig. 5(b)) thousands of Angstroms (macropore) in diameter, firstly, when it was heated under an oxygen-free atmosphere. As the temperature increased, the coking of the carbohydrates broke the glycoside bond of the glycan backbone that sectioned the cell wall as slice (Fig. 5(d)). Fragments with a cell wall thickness of several hundred Angstroms piled up and fused to form pores of several hundred Angstroms in diameter (macropore and mesopore). When the temperature was high enough, the amide bonds may break down. Peptide chains lengths of several tens of Angstroms tangled to form pores (Fig. 5(e)) several tens of Angstroms in diameter (mesopore). When the pyrolysis temperature was higher than 700°C, the bond between L-Ala, D-Glu, L-Lys and D-Ala broke to form the pore (Fig. 5(f)) of several Angstroms (micropore).

CONCLUSIONS

Results of element compositions indicated that carbon, hydrogen, and nitrogen concentrations were reduced as pyrolytic temperatures increased. The sulfur concentration, however, increased as the pyrolytic temperature increased. The ICP-AES and ICP-MS results indicated that the pyrolysis process concentrated the Al, Ca, Fe, Mg, K, Cu, Sr, and Sb. The pore size distribution analysis indicated that the pyrolytic residue of the biosludge was a mesopore. The highest BET surface area was obtained when the temperature and time were in the vicinity of 800°C and 30 min. The optimal pyrolytic conditions for micropore formation were in the vicinity of 800°C for 30 min and 900°C for 10 min. The results indicated that the bio-sludge could be an adsorbent resource under controlled pyrolytic temperature and time. The length of the molecular bond is used in the conceptual model to describe the development of pore volume. In a further study, we hope to modify the pyrolysis condition and treat the pyrolytic residue with chemicals to develop the pore volume to be an adsorbent.

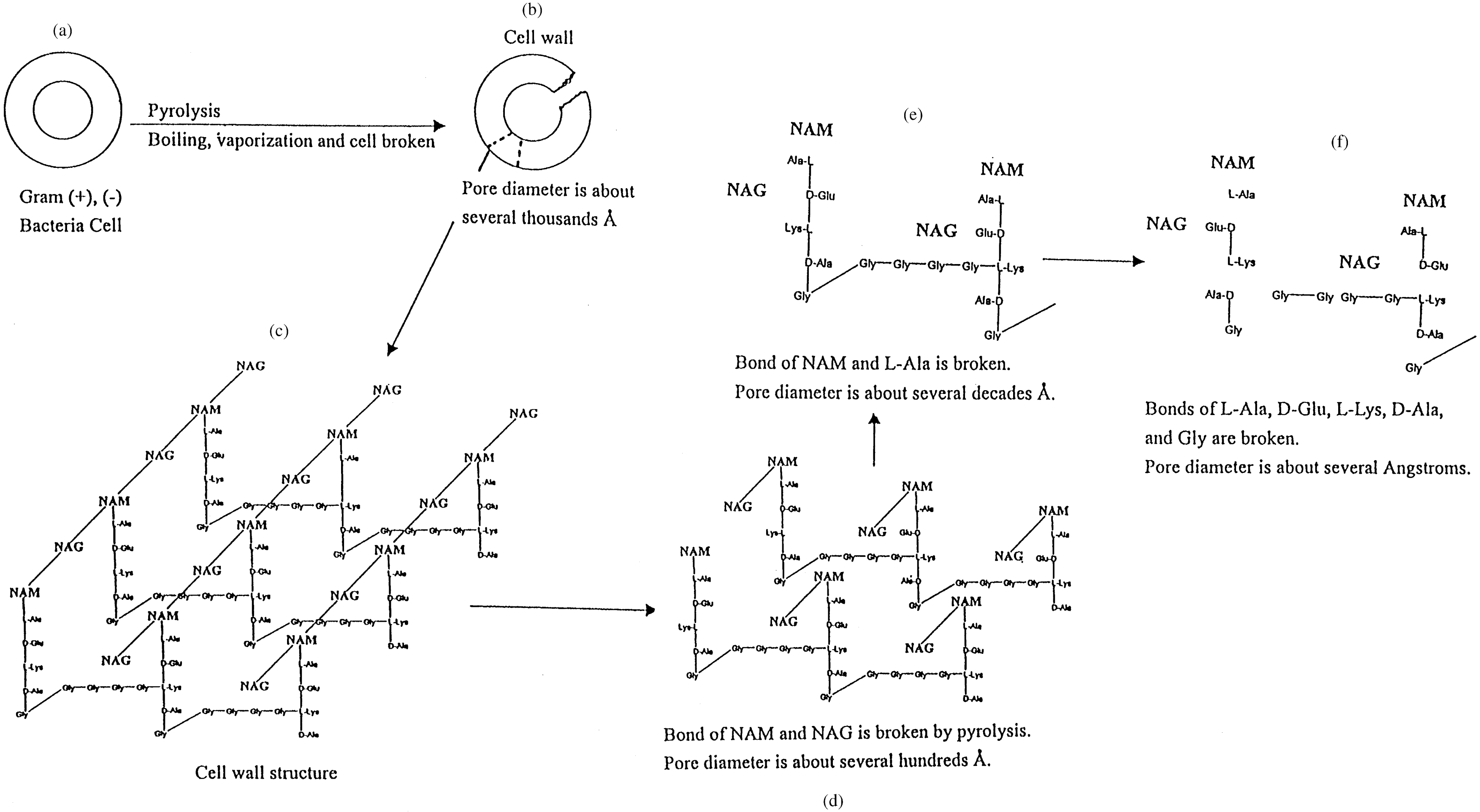

Fig. 5. Conceptual model of pore development for sludge pyrolysis.

Acknowledgements—The authors express their sincere thanks to the National Science Council, Taiwan, ROC (Contract No. NSC 89-2211-E-242-006) and the Ministry of Education for the financial support of this study.

REFERENCES

Barrett E. P., Joyner L. S. and Halenda P. P. (1951) The determination of pore volume and area distributions in porous substances. I. computations from nitrogen isotherm. *J. Am. Chem. Soc*. **73**, 373–380.

Bayer E. and Kutubuddin M. (1987) In *Low Temperature Conversion of Sludge and Waste to Oil*, eds K. J. Thome-Kozmiensky and U. Loll, pp. 314–318. EF Verlag, Berlin.

Bitton G. (1999) *Wastewater Microbiology*, 2nd ed. pp. 96–97, 187, Wiley, New York.

Bridle T. R. (1982) Sludge-derived oil: wastewater treatment implications. *Environ. Tech. Lett*. **3**, 151–156.

Brubauer S., Emmett H. P. and Teller E. (1938) Adsorption of gas in multimolecular layers. *J. Am. Chem. Soc*. **60**, 309–319.

Burkert U. and Allinger N. L. (1982) *Molecular Mechanics*. ACS, Washington, DC, USA.

Chiang P. C. and You J. H. (1987) Use of sewage sludge for manufacturing adsorbents. Can. *J. Chem. Eng*. **65**, 922.

Dumpelmann R., Richarz W. and Stammbach M. R. (1991) Kinetic studies of the pyrolysis of sewage sludge by tga and comparison with fluidized beds. *Can. J. Chem. Eng*. **69**, 953–922963.

Harkins W. D. and Jura G. (1944) Surfaces of solids XIII: a vapor adsorption method for the determination of the area of a solid without the assumption of a molecular area and the areas occupied by nitrogen and other molecules on the surface of a solid. *J. Chem. Phys*. **66**, 1366–1373.

Kaminsky W. (1989) Pyrolysis von biomasse. *Chem. Ing. Tech*. **61**, 775–782.

Kim B. R., Kalis E. M., Salmeen I. T., Kruse C. W., Demir I., Carlson S. L. and Rostam-Abadi M. (1996) Evaluation paint-sludge char for adsorption of selected paint solvents. *J. Environ. Eng*. **122**(6), 532–539.

Lippens B. C. and de Boer J. H. (1965) Studies on pore system in catalysts V. the t method. *J. Catal*. **4**, 319–323.

Lu G. Q., Low C. F., Liu C. Y. and Lua A. C. (1995) Surface area development of sewage sludge during pyrolysis. *Fuel* **74**(3), 344–348.

Piskorz J., Scott D. S. and Westerberg. (1986) Flash pyrolysis of sewage sludge. *I&EC Process Design Dev*. 25, 265–270.

Taiwan Environmental Protection Agency (1999) *Workshop of Wastewater Treatment Technology and Management System- Sludge Treatment, Reduction, and Emergency System, Taipei, Taiwan*, p. 70 (in Chinese).

Talaro Kathleen P. and Talaro A. (1999) *Foundations in Microbiology Basic Principles*. pp. 38–45, 88–100. McGraw-Hill, Boston.

Todar K. (1999) *Structure and Function of Procaryotic Cells*. http://www.bact.wisc.edu.tw/\\bact303\\Structure http://www.bact.wisc.edu.tw/\bact303\structure.